

Application of nanoporous silicon substrates for terahertz spectroscopy

Shu-Zee A. Lo,¹ Gagan Kumar,² Thomas E. Murphy,^{2,*} and Edwin J. Heilweil¹

¹Radiation and Biomolecular Physics Division, Physical Measurement Laboratory, National Institute of Standards and Technology, Gaithersburg, MD 20878, USA

²Institute for Research in Electronics & Applied Physics, University of Maryland at College Park, College Park, MD 20740, USA

*tem@umd.edu

Abstract: Mid to far-infrared (terahertz) spectroscopy is a valuable tool for probing and characterizing macromolecular structures and motions of complex molecules, including low frequency vibrational and phonon modes in condensed phases. We describe here an improved and readily implemented method for performing terahertz spectroscopic measurements by using a nanoporous silicon substrate to capture and concentrate the substance to be analyzed. We compare the results to conventional sampling methods, including dissolution and crystallization on a flat silicon surface and dispersing crystallites in compressed polyethylene pellets, and show that the use of a transparent, nanoporous substrate provides both increased sensitivity and yields sharper spectral features than conventional solid-state sampling approaches. FTIR measurements are reported over the spectral range from 50–2000 cm⁻¹ (1.5–60 THz), for salicylic acid, dicyanobenzene, glycine, and aspartame.

© 2012 Optical Society of America

OCIS codes: (300.6495) Spectroscopy, terahertz; (300.6270) Spectroscopy, far-infrared; (160.4236) Nanomaterials.

References and links

1. M. van Exter, C. Fattinger, and D. Grischkowsky, "Terahertz time-domain spectroscopy of water vapor," *Opt. Lett.* **14**, 1128–1130 (1989).
2. O. Esenturk, A. Evans, and E. Heilweil, "Terahertz spectroscopy of dicyanobenzenes: anomalous absorption intensities and spectral calculations," *Chem. Phys. Lett.* **442**, 71–77 (2007).
3. S. Kumar, A. K. Rai, V. Singh, and S. Rai, "Vibrational spectrum of glycine molecule," *Spectrochim. Acta* **61**, 2741–2746 (2005).
4. M. Kutteruf, C. Brown, L. Iwaki, M. Campbell, T. Korter, and E. Heilweil, "Terahertz spectroscopy of short-chain polypeptides," *Chem. Phys. Lett.* **375**, 337–343 (2003).
5. N. Peica, "Identification and characterisation of the E951 artificial food sweetener by vibrational spectroscopy and theoretical modelling," *J. Raman Spectrosc.* **40**, 2144–2154 (2009).
6. V. Volovšek, L. Colombo, and K. Furić, "Vibrational spectrum and normal coordinate calculations of the salicylic acid molecule," *J. Raman Spectrosc.* **14**, 347–352 (1983).
7. E. J. Heilweil and D. F. Plusquellic, "Terahertz spectroscopy of biomolecules," in *Terahertz Spectroscopy: Principles and Applications*, S. Dexheimer, ed. (CRC Press, 2008), pp. 269–298.
8. V. Meenatchi, K. Muthu, M. Rajasekar, S. Meenakshisundaram, and S. Mojumdar, "Crystal growth, structure and characterization of o-hydroxybenzoic acid single crystals," *J. Therm. Anal. Calorim.* **108**, 895–900 (2012).
9. M. Bhat and S. Dharmaprasanth, "Growth of nonlinear optical γ -glycine crystals," *J. Cryst. Growth* **236**, 376–380 (2002).
10. J. S. Melinger, N. Laman, S. S. Harsha, and D. Grischkowsky, "Line narrowing of terahertz vibrational modes for organic thin polycrystalline films within a parallel plate waveguide," *Appl. Phys. Lett.* **89**, 251110 (2006).

11. S. S. Harsha, J. S. Melinger, S. B. Qadri, and D. Grischkowsky, "Substrate independence of THz vibrational modes of polycrystalline thin films of molecular solids in waveguide THz-TDS," *J. Appl. Phys.* **111**, 023105 (2012).
 12. D. F. Plusquellic, K. Siegrist, E. J. Heilweil, and O. Esenturk, "Applications of terahertz spectroscopy in biosystems," *Chem. Phys. Chem.* **8**, 2412–2431 (2007).
 13. Certain commercial equipment, instruments or materials are identified here to adequately specify the experimental procedure. In no case does identification imply recommendation or endorsement by NIST, nor does it imply that the materials or equipment identified are necessarily the best available for the purpose.
 14. M. Franz, B. M. Fischer, and M. Walther, "The Christiansen effect in terahertz time-domain spectra of coarse-grained powders," *Appl. Phys. Lett.* **92**, 021107 (2008).
 15. S. Saito, T. M. Inerbaev, H. Mizuseki, N. Igarashi, and Y. Kawazoe, "Terahertz vibrational modes of crystalline salicylic acid by numerical model using periodic density functional theory," *Jpn. J. Appl. Phys.* **45**, 4170–4175 (2006).
 16. Y. Ueno and K. Ajito, "Terahertz time-domain spectra of aromatic carboxylic acids incorporated in nano-sized pores of mesoporous silicate," *Anal. Sci.* **23**, 803–807 (2007).
 17. J. Higgins, X. Zhou, and R. Liu, "Density functional theory study of vibrational spectra: 9. Structures and vibrational assignments of dicyanobenzenes," *Spectrochim. Acta A* **53**, 721–731 (1997).
 18. A. Bouchard, G. W. Hofland, and G.-J. Witkamp, "Solubility of glycine polymorphs and recrystallization of β -glycine," *J. Chem. Eng. Data* **52**, 1626–1629 (2007).
 19. X. K. Zhang, E. G. Lewars, R. E. March, and J. M. Parnis, "Vibrational spectrum of the acetone-water complex: a matrix isolation FTIR and theoretical study," *J. Phys. Chem.* **97**, 4320–4325 (1993).
 20. Y. Ueno, R. Rungsawang, I. Tomita, and K. Ajito, "Terahertz time-domain spectra of inter- and intramolecular hydrogen bonds of fumaric and maleic acids," *Chem. Lett.* **35**, 1128–1129 (2006).
-

1. Introduction

Far infrared (IR) or terahertz spectroscopy is an important diagnostic tool that can provide insight into low frequency vibrational and phonon modes of complex molecules and crystals. Applications include forensics, industrial process measurement, environmental monitoring, and chemistry research. One of the challenges with far infrared spectroscopy is finding a suitable substrate or host material that can support the substance to be analyzed without obscuring or impairing its absorption spectrum. Optical substrates that are commonly used in other spectral regimes are either opaque in the far infrared, or exhibit their own characteristic absorption features that must be removed from the measurement. Even when a transparent terahertz substrate, like semi-insulating silicon, is employed, a thin surface layer of analyte precipitated or deposited on the flat substrate is often too thin to produce significant absorption at long wavelengths. Aqueous solutions are equally problematic because water has strong absorption throughout the far infrared [1].

The most common method of preparing samples for far-infrared or terahertz spectroscopy is to grind the analyte into a dry, fine powder, mix it with polyethylene (PE) powder or potassium bromide (KBr), and compress the resulting mixture into millimeter-thick pellets. PE and KBr are used because they exhibit reasonably low loss, and few absorption bands across the mid- to far-infrared spectral regions. This approach has been used to measure the far-infrared or THz absorption spectra of a number of amino acids, crystalline peptides, proteins, nucleic acids and other biomolecules [2–7]. There is some evidence that the process of compression and consolidation can result in asymmetry, broadening and displacement of the absorption bands, compared to what is observed in bulk crystals [8, 9]. Moreover, the pressed pellet method requires a large volume of analyte and is often a time-consuming process that is incompatible with rapid, highly sensitive spectral analysis and monitoring.

Recently, waveguide-based spectroscopy methods have been demonstrated, in which a thin layer of analyte is precipitated onto one plate of a metallic waveguide or parallel plate transmission line [7, 10–12]. This leads to a stronger absorption spectrum compared to what would be obtained by transmission through a single layer, and a sharpening of features in comparison to results obtained in a pressed pellet.

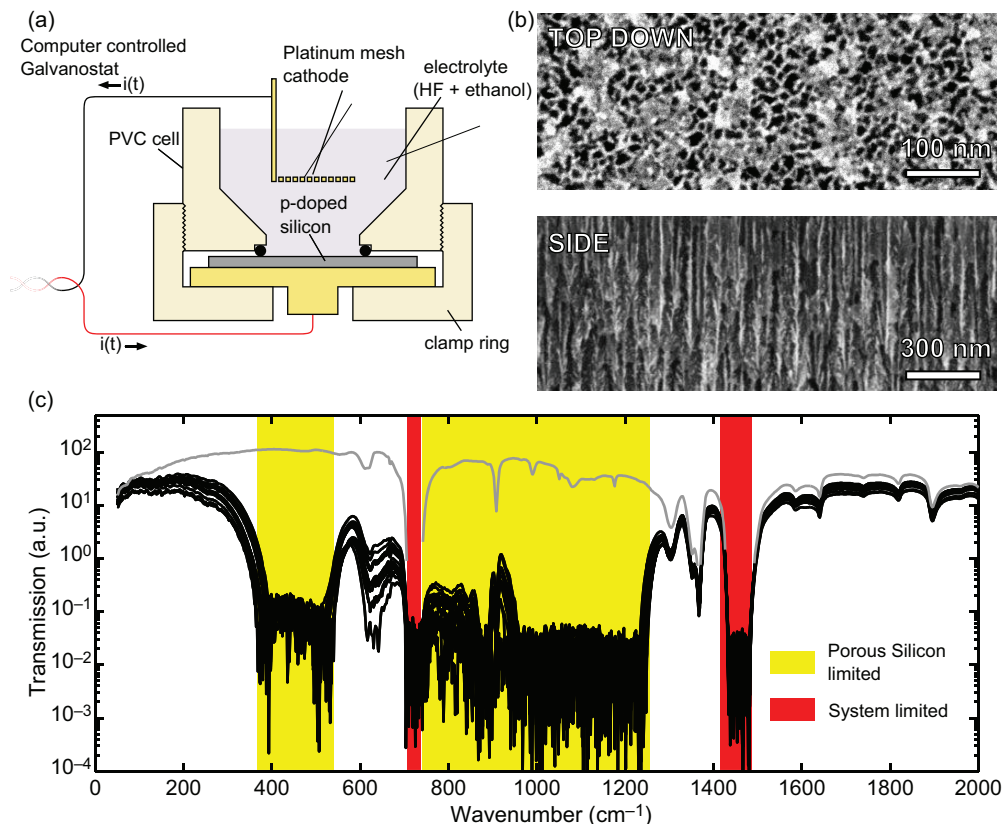


Fig. 1. (a) Diagram of the electrochemical etching system used to produce the porous silicon samples. (b) Scanning electron micrograph showing top-down and cross-sectional views of the porous silicon. (c) Transmitted signal from 15 separately fabricated porous silicon substrates, in comparison to the measured sample obtained with the sample removed. Yellow and red regions illustrate spectral regimes limited by the porous silicon substrate and the FTIR detector polyethylene window, respectively. The gray trace shows the system spectrum without a sample.

We present a novel method for terahertz spectroscopy that uses nanoporous silicon as a host substrate for capturing and collecting the analyte. Porous silicon is formed through electrochemical etching of crystalline silicon, a process that readily forms a thick optical material with nanometer pore size. One cubic centimeter of porous silicon can have as much internal surface area as a large tennis court. Such a nanoporous matrix will therefore allow a large quantity of surface-bound molecules to be distributed throughout an interaction volume that could be thicker than the wavelength - a tremendous advantage when conducting terahertz spectroscopy. Moreover, porous silicon is found to have several broad transparency windows in the mid- to far-IR spectral range, making it a suitable substrate for spectroscopy of a variety of substances. We compare the absorption spectrum measured using a porous silicon substrate to conventional pressed-pellet and surface evaporation/crystallization methods for four different molecules: salicylic acid, dicyanobenzene, glycine, and aspartame. We find that in cases where the molecules can be efficiently dissolved and deposited inside of the pores, smaller quantities of analytes are used and the absorption spectrum can be both sharper and more intense (all by as much as an order of magnitude, as is also found for the waveguide technique) than for the pressed-pellet or

surface precipitation methods.

2. Porous silicon fabrication

The porous silicon samples used in this study were fabricated using a process of electrochemical etching, beginning with double-side polished boron-doped silicon wafers with a resistivity of (5 – 20) m Ω cm. Figure 1(a) shows a diagram of the electrochemical etching system. One side of the silicon sample was pressed, using an o-ring gasket, against the bottom opening in an electrochemical cell, which was filled with a (1:1:2) mixture of hydrofluoric acid, water, and ethanol. A platinum mesh anode was immersed in the electrolyte, while the silicon substrate served as the cathode. A computer-controlled galvanostat (Amel 2049 [13]) was used to deliver the electrochemical current required for producing the porous silicon. The etching current density of 90 mA/cm² over an exposed area of 10 mm diameter was applied, in pulses of 100 ms duration, with a 300 ms pause between pulses to allow the electrolyte to equilibrate within the pores. These parameters were found to produce a volume porosity of approximately 65% and a typical pore size of 10-100 nm. After etching the porous layer to a depth of approximately 200 μ m, the current density was increased to 226 mA/cm² for 7 s, which causes the porous layer to separate from the underlying substrate, resulting in a free-standing porous sample. The samples were rinsed in ethanol, dried under nitrogen flux, and oxidized in a rapid thermal annealing furnace for 5 minutes at a temperature of 673 K, in order to passivate the silicon surface with a thin oxide layer. Figure 1(b) depicts representative top-down and cross-sectional scanning-electron micrographs of fabricated porous samples, showing both the nanometer texture of the material, and columnar structure of the pores.

The porous samples were measured in a conventional Fourier-transform infrared spectroscopy (FTIR) system (Nicolet Magna-IR 550 Series II [13]) with a standard globar source that was modified to incorporate a deuterium triglyceride sulfide pyroelectric detector with a polyethylene window capable of detecting wavenumbers from 50–2000 cm⁻¹ in transmission configuration. Figure 1(c) shows the measured background spectrum of the system, collected with and without a porous silicon sample inserted, measured over the range from 50-2000 cm⁻¹. The measurements were performed with the sample at room temperature, and after purging the sample chamber with water- and carbon-dioxide-free air. The red shading in Fig. 1(c) indicates spectral regions where the FTIR system (which includes polyethylene windows) does not provide sufficient throughput for absorption spectroscopy. The yellow regions indicate additional absorption bands introduced by the porous silicon. The absorption band from 360–1250 cm⁻¹ is caused by the oxidized and hydrogenated surface of the porous silicon. The two absorption bands from 700–760 cm⁻¹ and 1410–1490 cm⁻¹ are attributed to the polyethylene window in the FTIR system.

3. Sample preparation and measurement

Figure 2 illustrates how the porous samples were loaded with analyte prior to measurement. The analyte was first dissolved in a solvent of either acetone or an acetone/water mixture (depending on the solubility of the analyte), and the resulting solution was deposited onto the top surface of the porous silicon using a micropipet. To ensure penetration of the solvent through the pores, the porous silicon was held via a weak vacuum applied to the back-side on an o-ring assembly, as shown in Fig. 2. The vacuum serves to both hold the sample and also draw the solution through the porous membrane. The back-side vacuum was found to be essential to prevent uncontrolled accumulation or runoff of the solution across the porous surface. After the loading process (detailed in next section), the sample was dried under continuous vacuum flow for 10 minutes. Successful penetration of the analyte through the porous layer was verified by visually observing precipitate on the back-side of the sample. Before spectroscopic measurement, the

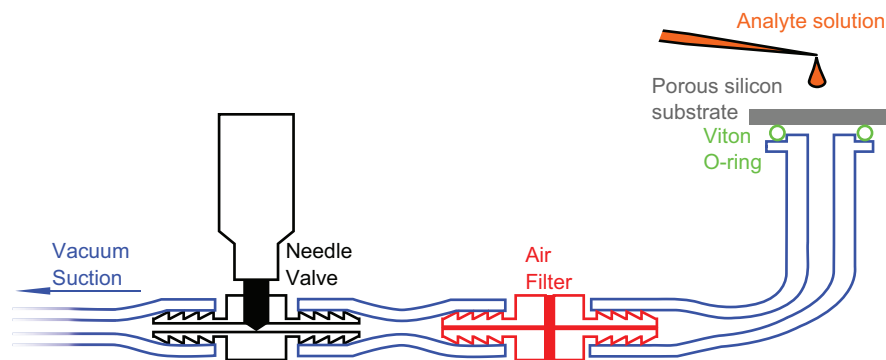


Fig. 2. Diagram of fixture used to apply solutions for crystallization within porous silicon substrates. A droplet of the analyte (dissolved in a suitable solvent) is deposited onto the front surface of the porous silicon, and drawn into the porous template by a weak vacuum applied to the back side of the sample.

front and back sides of the porous sample were gently cleaned with acetone or deionized water and lens paper, which removed remaining precipitate from the surface.

For comparison, we also prepared polyethylene pellet samples for each analyte examined in this work. Prior to preparing the pressed pellet samples, the dry analyte was ground into a fine powder with an average particle size smaller than $100\ \mu\text{m}$, as measured by optical microscopy. This step was found to be essential to prevent excessive scattering. For the pressed pellet measurement, 7 mg of ground analyte powder was mixed with 100 mg of polyethylene powder (Micro-Powder Inc. [13]) and compressed into a pellet of 13 mm diameter and approximately 2 mm thickness under an applied pressure of 275 kPa.

As an additional comparison, we prepared samples by dropping each analyte solution onto the polished surface of a nominally undoped, $280\ \mu\text{m}$ thick silicon wafer. A 10 mm diameter o-ring assembly was mounted against the front of the flat silicon in order to confine the analyte to a region comparable to that of the porous sample, while preventing uncontrolled spillage or runoff. The sample was allowed to dry in the room temperature ambient environment, leaving a 10 mm diameter surface residue. To facilitate comparison, the mass of the deposited analyte was adjusted to be equivalent to the amount introduced into the porous silicon sample.

All samples were measured in the FTIR at room-temperature, over a spectral range from $50\text{--}2000\ \text{cm}^{-1}$, with a spectral resolution of $4\ \text{cm}^{-1}$ and 128 scans averaged. For the polyethylene pellet cases, the absorption spectrum was obtained by computing the ratio of the measured signal to that obtained from a similarly made pure polyethylene pellet. For porous silicon and flat silicon substrates, the absorption spectra were obtained by referencing to previously unloaded spectra of the same porous silicon and flat silicon substrate.

4. Measurements

For the salicylic acid measurements, 100 mg of dry salicylic acid, in powder form (Sigma Aldrich [13]) was dissolved in 10 ml of acetone. $100\ \mu\text{L}$ of the resulting solution was deposited onto the porous silicon surface, using the method described above and depicted in Fig. 2. After evaporation of the solvent, this corresponds to at most 1 mg of pore-incorporated salicylic acid, not accounting for the residue that was wiped from the front and back surfaces of the porous sample after loading.

Figure 3 compares the measured absorption spectrum for the salicylic acid from the three

different samples: porous silicon, flat silicon, and pressed pellet. Although the porous silicon contains at most 1 mg of salicylic acid, compared to 7 mg in the pressed pellet of comparable diameter, we observe a significant increase in the spectral absorption feature peak intensities in the porous template. We note that, to facilitate comparison, the porous silicon spectrum was plotted on a different vertical scale. For example, the absorption peak at 1670 cm^{-1} is more than $10\times$ stronger than that observed in the polyethylene pellet, and is limited by the dynamic range of the instrument. An interesting feature of the porous silicon result is that the absorption peaks appear sharper and more clearly defined than in the pressed pellet, even though the instrument spectral resolution was identical for both measurements. For example, the full-width at half-maximum of the absorption peak at 282 cm^{-1} is 18 cm^{-1} for the pressed pellet case, compared to 11 cm^{-1} for the porous silicon case. The width estimate is limited by the FTIR scanning resolution of 4 cm^{-1} . The peaks at 660 cm^{-1} show a similar narrowing. Some of the peak broadening observed in the polyethylene pellet could be attributed to scattering by analyte particles embedded in the polyethylene [14], an effect that is absent in the nanoporous material because of the small particle size. The measurements obtained by deposition on a flat silicon wafer are consistent, but the corresponding feature absorptions are always found to be much weaker and often broader than both the pressed pellet and porous silicon spectra. An explanation for this generalization is that rapid crystallization on the silicon surface induces a variety of polymorphic or inhomogeneous structures that broaden and weaken the absorption features, making them more difficult to observe.

While the three absorption spectra show overall similar features, it is interesting that in the low wavenumber regime (below 100 cm^{-1}), some spectral features are absent in the porous silicon spectrum. The absorption behavior in this regime is thought to be dominated by low frequency phonon modes such as intermolecular hydrogen bonds, dimer bending, and lattice translation and rotation [6, 15]. In particular, the peak at 75 cm^{-1} is clearly seen in both the polyethylene and flat silicon samples, but is absent in the case of porous silicon. In a recent paper, Ueno and Ajito reported a similar finding with salicylic acid in mesoporous silicate using terahertz spectroscopy [16]. The potential explanation offered was that these absorption features are inhibited due to the constrained intermolecular interaction or lattice movement inside the confining structure – a hypothesis that seems to be further supported by our observations. The columnar nature of the nanoporous template, together with the transverse direction of the incident electric field could further diminish the relative absorption strength of these modes. Another possibility is that nanopore confinement induces crystalline orientation and hence changes in relative feature intensities compared to random crystallite orientations in the pellet or deposited on the silicon wafer surface. Further studies obtaining polarized FTIR spectra would help distinguish between these two possibilities.

We also conducted similar measurements using two isomers of dicyanobenzene, structurally depicted in Fig. 4. Powder of 1,3- and 1,4-dicyanobenzene (Sigma Aldrich [13]) was dissolved in acetone at concentrations of 11.78 mg/ml and 11.10 mg/ml , respectively. On both flat and porous silicon substrates, we loaded $50\text{ }\mu\text{l}$ onto the substrates, corresponding to an estimated analyte weight of $0.5\text{--}0.6\text{ mg}$. For comparison, the pressed pellet and flat silicon samples were prepared as described earlier.

As with the case of salicylic acid, at wavenumbers above 500 cm^{-1} , the absorption features are sharper and stronger than those observed in the polyethylene pellets, and much more easily observed than on the flat silicon surface. For the polyethylene pellet cases, thickness differences between pellets loaded with the isomers of dicyanobenzene and the reference polyethylene pellet introduced artificial dips in absorption. For the flat silicon measurements, the large index of refraction difference between the substrate and surrounding air causes multiple internal reflections inside of the substrate, leading to the Fabry-Pérot response seen in Fig. 4. In general,

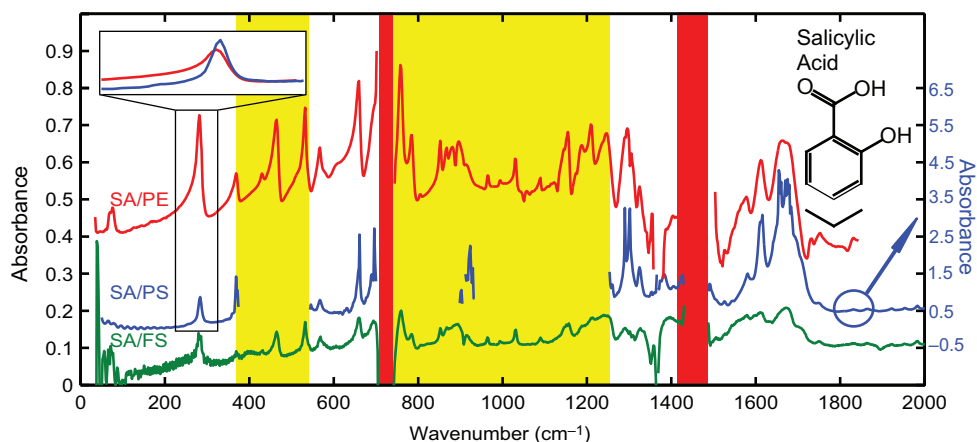


Fig. 3. Absorption spectra of salicylic acid loaded into a conventional polyethylene pellet (red line), porous silicon (blue line) and deposited on an intrinsic silicon wafer (green line). The absorbance of the salicylic acid pellet is shifted vertically for clarity. Oscillation of the flat silicon case in the low wavenumber regime ($< 300\text{cm}^{-1}$) is due to the Fabry-Perot resonances of the flat silicon wafer substrate. As with Fig. 1, yellow regions delineate spectral regimes limited by absorption of the substrate while the red regions depict spectral regimes limited by the FTIR system. Inset: enlarged plot of spectral line at 282cm^{-1} , comparing the line shape for the pressed pellet and porous silicon.

although the analyte mass deposited in the porous silicon is less than 10% of that contained in the polyethylene pellet, the absorption features are comparable in absorbance and correspond well to results reported previously in the literature [2, 17].

We next turn to glycine, the simplest amino acid contained in a wide variety of proteins in consumer and pharmaceutical contexts. Compared with salicylic acid and dicyanobenzene, the ionic solution structure of glycine does not readily dissolve in acetone, which poses a challenge for porous silicon spectroscopy. Although glycine is readily soluble in water, the front surface of the oxidized porous silicon surface is hydrophobic, making it difficult to completely pull an aqueous solution through the pores, even with vacuum back-pressure applied. Moreover, once water becomes trapped inside the pores it becomes difficult to drive it out, leading to increased substrate absorption. To mitigate this effect, we used a solvent mixture of acetone and water, in a 1:1 volume ratio. Dry glycine powder (ICN Biomedical Inc. [13]) was added to the mixture until the solution was saturated. The saturated solution of glycine in water and acetone was dispensed onto the porous silicon and flat silicon as described earlier, and the sample was left to dry in an ambient environment. Based upon the published solubility of glycine in acetone and water [18], we estimate the weight of glycine contained in the $100\ \mu\text{l}$ droplet dispensed on the sample to be approximately $2.4\ \mu\text{g}$.

While the flat silicon sample dried rapidly under ambient conditions, the absorption spectrum of the porous sample required many hours to stabilize. This evolution is shown in Fig. 5(a), which shows the absorption spectrum measured at 10 mins, 20 mins, 18 hrs, and 5 days following sample preparation. Even though the weight of the analyte is less than 0.1% of that contained in the pressed pellet, most of the absorption features are comparable in amplitude, and the mid wavenumber ($> 800\text{cm}^{-1}$) absorption features are somewhat sharper than those observed for the pellet. In some cases, the peaks are found to shift and sharpen as the sample dries. The overall spectral shape agrees well with previously published and theoretically predicted results [3, 4].

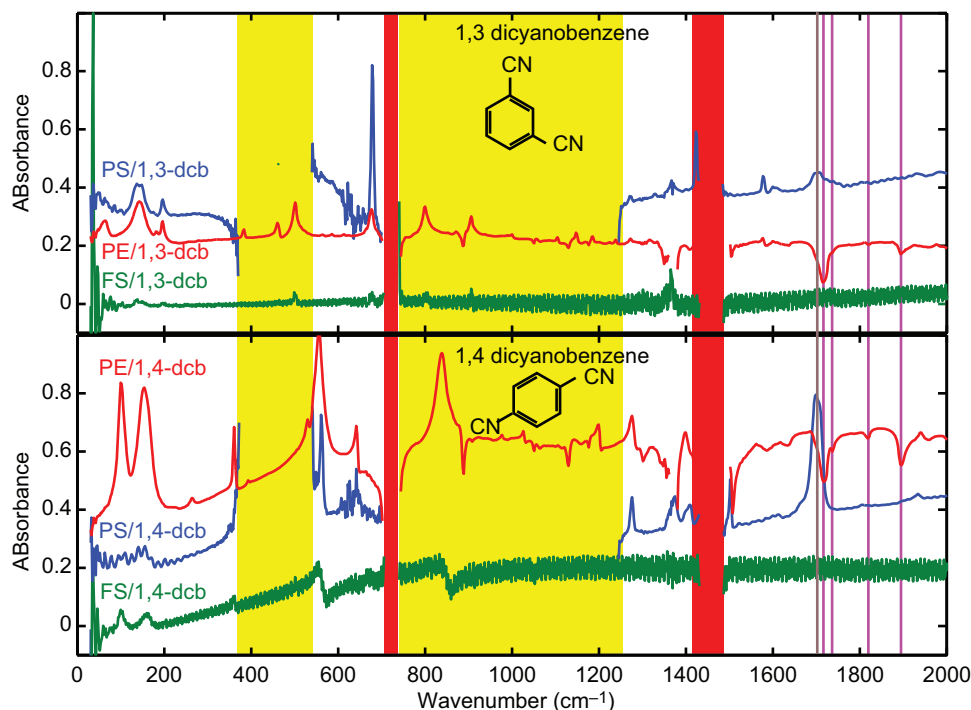


Fig. 4. Comparison between polyethylene pellet (Red), porous silicon (Blue) and flat silicon (Green) loaded with 1,3-dicyanobenzene and 1,4-dicyanobenzene. Porous silicon and polyethylene results are shifted vertically for clarity. Gray lines correspond to absorption peaks of residual acetone on the porous silicon substrates while purple lines delineate cancellation artifacts for polyethylene pellets. Yellow and red regimes illustrate porous silicon and system limited regimes as in Fig. 1(c).

The evolving absorption spectrum for this sample can be explained by a slow drying process in the nanoscale silicon template, in which a portion of the solvent remains trapped inside of the porous matrix for hours or days. To illustrate this, in Fig. 5(b), we plot the measured absorption spectrum for a porous substrate that was loaded with pure water:acetone solvent, without glycine. The prominent absorption features associated with absorbed water (e.g., broad feature near 200 cm^{-1} and sharper one near 1600 cm^{-1}) are observed to diminish as the solvent slowly evaporates from the porous substrates. Because the post-treated, oxidized silicon nanoporous substrate contains bridging oxygen and dangling hydroxyl groups, hydrogen-bonded water is extremely difficult to remove unless heating and vacuum treatment is used. Trapped water can also significantly change the crystallinity or become incorporated into analyte crystal structure, affecting observed terahertz spectra. Again, the periodic spectral absorption pattern observed at low wavenumber is associated with a Fabry P erot resonance of the porous sample.

As a final test case, we considered the artificial sweetener aspartame. Like glycine, aspartame is highly insoluble in acetone, and we therefore used a (1:1) volume mixture of acetone and water in order to balance competing demands for solubility and penetrability in the porous silicon. For these measurements, 26.9 mg of dry aspartame powder (Supelco [13]) was dissolved into a 10 ml mixture of acetone and water with volume ratio of (1:1). The resulting mixture was heated to 313 K and mixed under ultrasonic agitation for 30 minutes. 50 μl of the resulting solution was deposited onto the porous silicon and flat silicon substrates. The weight

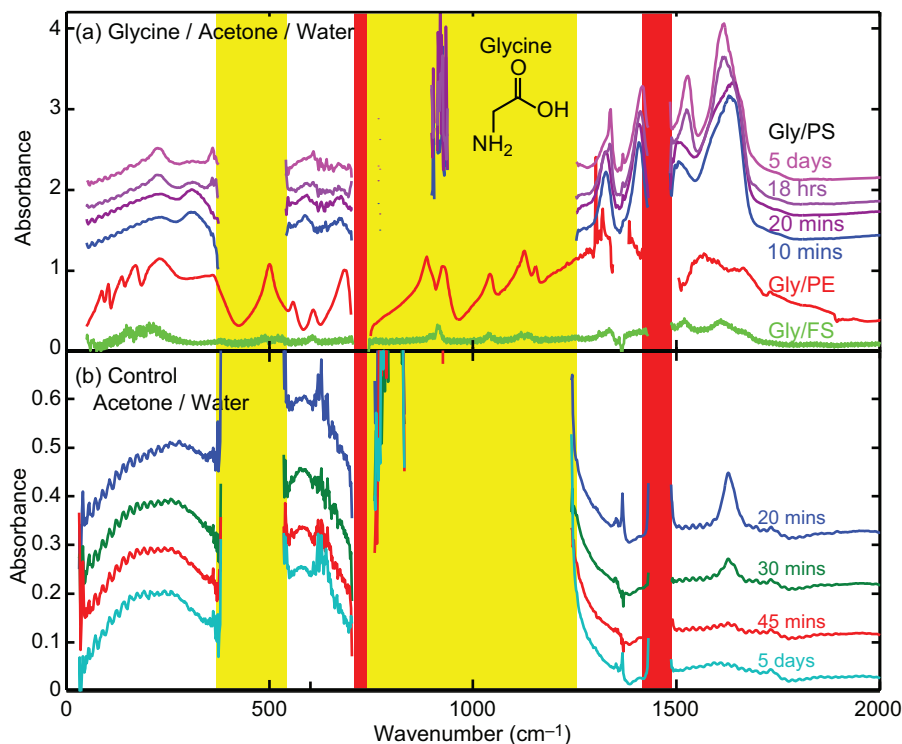


Fig. 5. (a) Absorption spectra of glycine loaded into a polyethylene pellet (red line), porous silicon (blue to purple lines) and on an intrinsic silicon wafer surface (green line). As with Fig. 3, the yellow and red regions delineate low signal regimes due to absorption bands of porous silicon and the FTIR polyethylene window. Oscillation in the intrinsic silicon case is due to Fabry-Perot resonances. Spectra are shifted vertically for clarity. As water:acetone solvent evaporated from the porous silicon substrate, some glycine absorption features shifted and sharpened while others emerged or diminished. (b) Porous silicon loaded with the same volume of acetone:water mixture. Absorption features of the control clearly explain the observed changes of absorption features for porous silicon loaded with glycine/acetone/water.

of the deposited analyte was estimated to be 0.13 mg for the flat silicon and porous samples. Absorption spectra were measured several days after loading, to allow adequate time for the solvent to fully evaporate from the pores. Figure 6 compares the absorption spectrum obtained with the porous silicon to that of a pressed pellet. The porous silicon measurement agrees well with the pellet measurement and with published data [5] in the regime of 1500–2000 cm^{-1} . Below 700 cm^{-1} , the absorption features of aspartame were obscured by the broad absorption features of absorbed solvent, which is retained in the sample. The absorption features of the same amount of aspartame loaded on flat silicon were too small to be detected by the FTIR and are therefore not shown here. In contrast with the three other analytes considered here, the absorption features of aspartame in porous silicon appeared to be broadened in comparison to the pressed pellet measurements. We attribute the discrepancy to the presence of residual solvent trapped in the porous template, which, in the case of aspartame, was not easily removed through conventional static drying means.

This result highlights one of the key challenges of using nanoporous materials for terahertz spectroscopy – while water is one of the most commonly used solvents for many biological

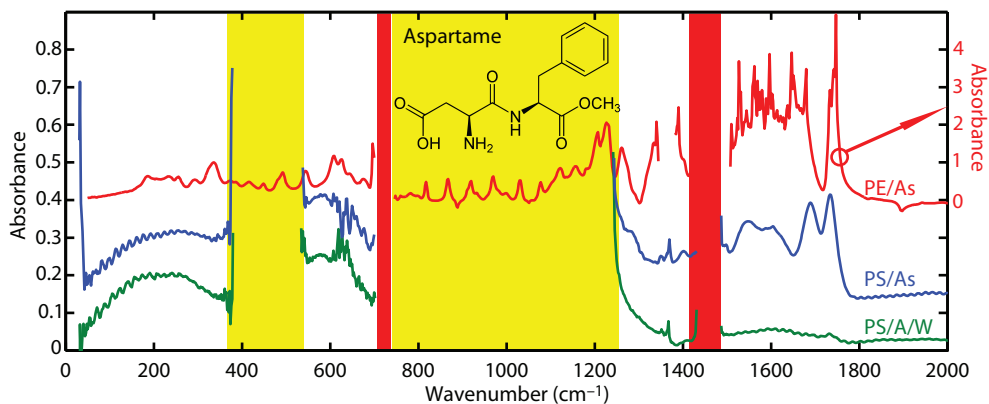


Fig. 6. Comparison between the polyethylene pellet with aspartame (blue line), porous silicon loaded with aspartame/acetone/water (red line) and acetone/water (green line) after equilibrium has been reached.

analytes, it is challenging to fill the nanometer-scale pores with aqueous solution, and equally difficult to drive off the solvent once it is there.

To investigate the scalability and spectral linearity of the method, we performed experiments in which successive drops of analyte were applied sequentially to the same porous silicon sample, while monitoring the absorption spectrum after each drop was applied. For this study, we dissolved 21 mg of salicylic acid into 10 ml of acetone. The solution was applied to a porous silicon substrate in 10 μ l drops (21 μ g of salicylic acid), and after each drop the sample was dried and the absorption spectrum measured. Figure 7(b) shows the sequence of spectra obtained after 1-9 sequentially added drops. Figure 7(a) plots measured absorbance of the seven dominant absorption peaks of salicylic acid as a function of the applied dose. In all cases, the absorbance scales approximately linearly with the volume of analyte, as expected.

As a further control experiment, we conducted the same measurements using pure acetone, Fig. 7(c). While some residual absorption peaks associated with acetone are still observed, they remain at a very low, constant level and do not increase with successive drops. The two absorption peaks in the spectrum, 1375 cm^{-1} and 1691 cm^{-1} , correspond to known acetone/water complex absorption peaks [19] and can hence be attributed to residual water and acetone on the pore surface.

5. Conclusion

We have evaluated the potential application of crystalline porous substrate materials for use in infrared absorption vibrational spectroscopy. It was found that the porous silicon substrate used in this experiment has indeed enhanced and in many cases sharpened the higher energy absorption modes for several crystallized organic and biological analytes. For low energy modes the absorption features appear to remain relatively broad and unamplified. We attribute this discrepancy to a reduction of intermolecular interaction, which lead to the reduction of intermolecular and lattice modes usually dominant in the low wavenumber regime. This characteristic of porous substrate was also observed by Ueno et. al. for multiple analytes [16, 20].

Although this work is conducted using a polyethylene equipped FTIR detector window and Si-coated mylar beamsplitter (designed for the $< 400 \text{ cm}^{-1}$ far-IR region) and polyethylene pellets, we also noted that the choice of using polyethylene introduced several artificial features in analyte pellet absorption spectra. In the ideal situation, the spectral range of $> 400 \text{ cm}^{-1}$

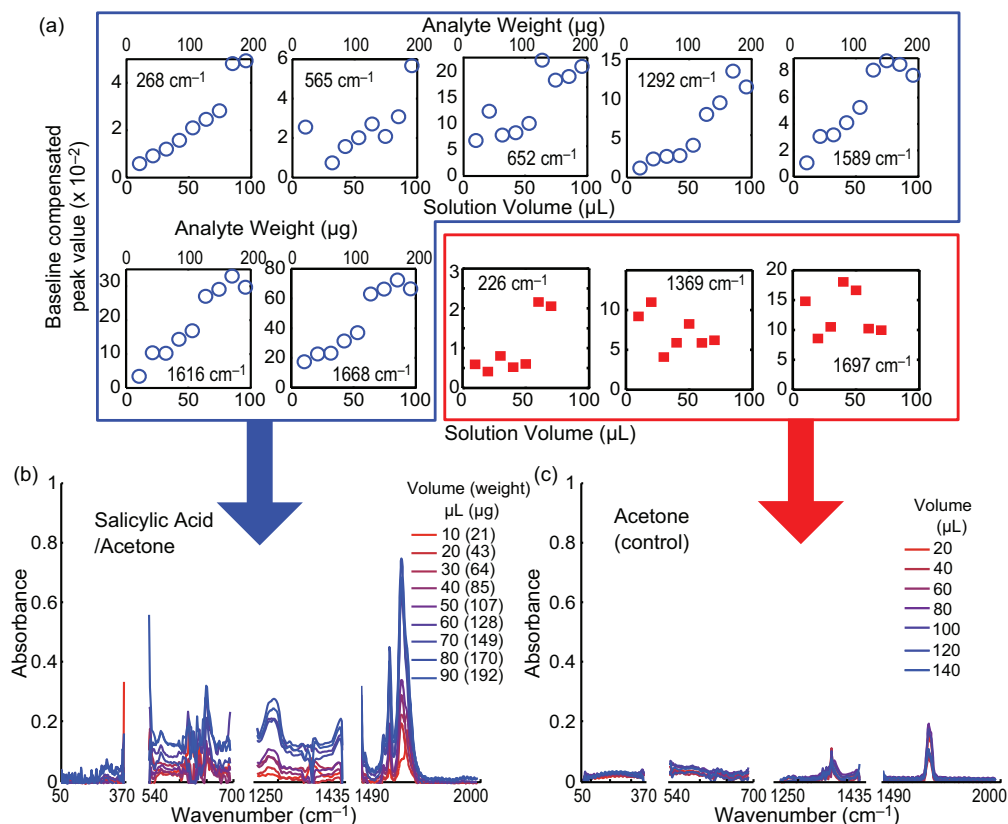


Fig. 7. Variation of the absorption features of salicylic acid/acetone and pure acetone versus the accumulated volume of the analyte dropped onto a porous silicon substrate. (a) Baseline compensated peak values for salicylic acid/acetone (blue opened circles) and pure acetone (red closed squares). (b) Corresponding salicylic acid/acetone absorption features. The legend contains the dropped analyte volume (calculated analyte weight) for each successive addition. (c) Corresponding solvent-only control experiment on the same absorbance scale. The legend contains the dropped acetone volume.

should be measured with a standard KBr beamsplitter equipped FTIR system.

One potential setback for this method is that the absorption features of the substrate can obstruct or interfere with measuring absorption features from the analyte. However, it may be possible to extend this idea to other porous materials with more favorable transmission properties (e.g., GaAs, SiC, SiN, etc.). Furthermore, absorption by the substrate could be significantly reduced by using a thinner substrate. Such use would not significantly impact the experiment, as only micrograms of analyte are apparently required for terahertz absorption spectroscopy work.

The effect of residual solvent in the porous silicon substrate clearly affects the crystallization properties of analytes, as shown by these measurements, especially when aqueous solutions are used. This drawback could potentially be alleviated by applying better environmental control of the FTIR sample chamber. In addition to polarization and sample orientation studies, we are also currently investigating the possibility of enclosing the sample inside a temperature-controlled vacuum cryostat to carefully drive out residual solvent and monitor spectral feature changes during the drying and crystallization process.

Acknowledgments

This work was partially supported by NIST financial assistance award number 70NANB12H009, NSF CBET award 0932673, and the Office of Naval Research, through the University of Maryland Center for Applied Electromagnetics (Grant No. N000140911190). The authors also thank Dr. Zeeshan Ahmed for his advice on sample preparation.